Investigation of Orientation Estimation of Multiple IMUs

Simone A. Ludwig

Department of Computer Science,
North Dakota State University,
Fargo, ND, USA
E-mail: simone.ludwig@ndsu.edu

Inertial Measurement Units (IMUs) were first applied to aircraft navigation and large devices in the 1930s. At that time their application was restricted because of constraints such as size, cost, and power consumption. In recent years however, Micro-electromechanical (MEMS) IMUs were introduced with very favorable features such as low cost, compactness, and low processing power. One of the disadvantages of these low cost IMU sensors is that the accuracy is lower compared to high-end sensors. However, past experimental results have shown that redundant MIMUs (Magnetic and Inertial Measurement Units) improve navigation performance such as for unmanned air vehicles. Even though past simulation and experimental results demonstrated that redundant sensors improve the navigation performance, however, none of the current research work offers information as to how many sensors are required in order to meet a certain accuracy. This paper evaluates different numbers of sensor configurations of an MIMU sensor array using a simulation environment. Differently rotated MIMU sensors are incrementally added and the Madgwick filter is used to estimate the Euler angles of foot mounted MIMU data. The evaluation measure used is the root mean square error (RMSE) based on the Euler angles as compared to the ground truth. During the experiments it was noticed that the execution time with increasing number of sensors increases exponentially, and thus, the parallelization of the code was designed and implemented, and run on a multi-core machine. Thus, the speedup of the parallel implementation was evaluated. The findings using the parallel version with sixteen sensors are that the execution time is less than twice the execution time of having only 1 sensor and 24 times less than using the sequential version with the added benefit of a 26% increase in accuracy.

Keywords: IMU; Madgwick filter; Multi-core processing; performance evaluation.

1. Introduction

Inertial Measurement Units (IMUs) were first applied to aircraft navigation and large devices in the 1930s.[1] However, the application at that time was restricted because of its constraints that were mainly due to size, cost, and power consumption. Recently, Micro-electromechanical (MEMS) IMUs were introduced with very favorable features such as low cost, compactness, and low processing power.[2] The everyday environment demands more and more advanced sensory systems and thus many researchers make use of more information regarding for example the current position and movements of people and objects to advance current systems and technologies.

The recent trend seen is that people make use of their own small electronice devices such as smart phones, GPS devices, and portable radios and the position information of the position sensors in those devices is used. Thus, the usage of IMUs have been increasing steadily over the years also since a wide variety of applications and systems are using them to measure movements in terms of acceleration, angular velocity, and rotation.[3]

One particular area where IMUs are also used is in UAVs (Unmanned Air Vehicles). The emergence of these low-cost IMUs allow them to be integrated into unmanned vehicles for agricultural applications such as precision farming and real-time irrigation control.[4,5] Moreover, given the current trend of modularization in unmanned system design, researchers and developers can use a relatively inexpensive commercial off-the-shelf IMU as part of the navigation system or develop their own system with those low-cost inertial sensors.

Other areas of usage of IMU as part of UAVs are indoor/outdoor mapping,[6] target tracking,[7] and industrial inspection.[8] MEMS IMUs are widely used as a low-cost option of attitude determination and short term position tracking through dead reckoning. However, without frequent corrections from a positional tracking system, such as GPS, they suffer from large drifts due to noise and repeated integrations of linear and rotational accelerations. GPS however suffer natural signal blockages from the environment such as tunnels, canyons and dense foliage or due to malicious GPS jamming and spoofing.[10] Thus, more and more applications that include GPS also integrate IMUs.

This paper seeks to determine if combining multiple MEMS IMUs in varying configurations has a significant ef-

fect on reducing the drift of the system. Furthermore, the influence of different numbers of sensors of an MIMU sensor array is evaluated. Thus, ground truth acceleration, rotation, and magnetometer data is used. This data is randomly rotated to simulate each IMU's location in the system as well as noise and bias are added as specified in.[11] The readings from each sensor in the virtual frame are averaged and the resulting accelerometer, gyroscope, and magnetometer measurements are fused in the Madgwick filter to obtain an orientation estimate. The root mean square error (RMSE) is calculated based on the estimated Euler angles and compared to the orientation RMSE of a single IMU centered at the origin of the system. In addition, the parallelization of the code is done using multiple cores (parallel) instead of only one core (sequential) in order to speed up the Euler angle estimation of the Madgwick filter and to investigate the effect of the scaling of the number of sensors. Thus, the execution times are recorded in order to show the efficiency of the parallel over the sequential implementation.

2. Related Work

Traditionally, multi-sensing systems have relied on complicated geometries. The main reason of having redundant sensors is to provide highly reliable and accurate sensor data and also reconfigure sensor network systems if some sensors failed. These two reasons provide the foundation for the design of fault-tolerant navigation systems in order to achieve reliability and integrity of inertial navigation systems.[12,13]

When considering the sensor shape configuration, past research identified two main approaches: orthogonal and non-orthogonal configuration. The non-orthogonal configuration uses a skewed setup whereby the measurement sensed by one sensor can be decomposed into three components along the orthogonal axes. The use of the non-orthogonal configuration has shown needing fewer sensors with the same accuracy compared to the orthogonal configuration that has been traditionally been used in fault-tolerant navigation system.[14]

Current optimization approaches involve factory calibration and this increases the cost of an MIMU substantially (as quoted in[15] the costs are around $1,000 per unit). Therefore, adding additional sensor triads or sensor arrays is economically viable if expensive calibration can be avoided.

One problem of low-cost sensors is that they are prone to large systematic errors (e.g., biases, scale factors, drifts), which limit their applicability even in integrated navigation systems. Thus, redundant sensors offer the possibility to efficiently enhance the navigation performances and particularly the orientation. First experiments undertaken have shown an improvement of navigation performance ranging from 30% to 50% when 4 sensors instead of 1 sensor are used.[16]

IMUs provide the orientation of a tracking object , however, it is not directly measurable. It has to be estimated from several correlated states such as angular rates measured by a gyroscope, linear acceleration measured by an accelerometer, and magnetic fields measured by an magnetometer. Thus, the estimation accuracy heavily relies on the sensor fusion algorithm used. Past research using IMUs have addressed the state estimation problem using nonlinear filtering techniques.[17] Different types of Kalman filters are widely using in the UAVs and related area.[18] One of the shortcomings is that many of these algorithms were developed for highly accurate inertial sensors. Those algorithms usually have high demands for computation power, which makes the use of low-cost IMUs ever more appealing. Since this paper is concerned with sensor fusion algorithms that are based on low-cost IMUs related work is summarized as follows. State estimation filters for low-cost IMUs is provided with several representative examples such as complementary filters,[19] extended Kalman filters,[20–22] and other nonlinear filters.[23]

Past research by the author applied the different filtering algorithms. In,[24] three filters were compared namely Madgwick and Mahony and a basic fusion approach. Foot mounted MIMU data was used to estimate the Euler angles as well as the position. The results showed that Madgwick obtains better heading orientation than Mahony and the basic AHRS approach in terms of the error (RMSE) of the Euler angles when compared to the ground truth. In,[25] the Madgwick and Mahony filters were compared with and the Extended Kalman Filter (EKF). Another work was concerned with the EKF filter addressing the shortcoming of the filtering solution becoming very poor when abrupt acceleration motions occur.[26] Thus, this was addressed using an optimization algorithm as a dynamic model correction. Better orientation estimates were achieved with this approach compared to the basic EKF approach. Something that was noted while conducting the different experiments with the different filters were that the execution time or runtime of the approaches are in need of improvement, which is the aim of this paper. Thus, a parallel implementation was done and evaluated on a multi-core machine. Speedup experiments were conducted to evaluate the performance gain achieved by the parallel implementation.

Although experimental results have demonstrated that redundant MEMS-IMUs integrated with GPS are an efficient way to improve navigation performances, the precise relationship between the number of sensors employed and the accuracy enhancement remains unclear.[27] Though simulations and experimental results have demonstrated that redundant sensors improve navigation performance[28–31] none of the work offers guidance as to how many sensors are required in order to meet certain specification and accuracy. Thus, more extensive simulation experiments are needed to analyze the improved accuracy as well as to analyze the execution time with increasing numbers of sensors.

3. Background to Magnetic and Inertial Measurement Unit (MIMU)

The Magnetic and Inertial Measurement Unit (MIMU) consists of MEMS (Micro-Electro-Mechanical Systems) sensors containing a 3-axis accelerometer, a 3-axis gyroscope, and a 3-axis magnetometer. The sensor outputs of these low-cost sensors are unfortunately not very good and thus suffer from problems such as noise, bias, scale factor, axis misalignment, axis non-orthogonality and local temperature.[32]

3.1. *Gyroscope*

The gyroscope measures the angular velocity of the tracking object in $\frac{rad}{s}$ and is represented by: $[s_{w_x} \quad s_{w_y} \quad s_{w_z}]^T$. Unfortunately, the gyroscope measurements suffer from:

- angular random walk
- bias instability
- rate random walk

The continuous time model for a gyroscope is expressed as:

$$s_w = s_{w_r} + s_{w_b} + s_{w_n} \tag{1}$$

where s_w is the angular rate measured by the gyroscope, s_{w_r} is the true angular rate, s_{w_b} is the gyroscope bias that models its derivative by a random walk noise, and s_{w_n} is the white noise of the gyroscope.

Since the gyroscope measurements are not enough for attitude estimation thus additional sensors such as accelerometers and magnetometer can be added and used to compensate this drift. The accelerometer corrects the pitch and roll angles whereby the magnetometer improves the yaw angle.

3.2. *Accelerometer*

The accelerometer measures the sum of the gravity and external acceleration of the tracking object in $\frac{m}{s^2}$. The acceleration is given as $s_a = [s_{a_x} \quad s_{a_y} \quad s_{a_z}]^T$. The three main types of noise are:

- velocity random walk
- bias instability
- correlated noise

The continuous time model of the accelerometer is as follows:

$$s_a = s_{a_r} + s_{a_b} + s_{a_n} \tag{2}$$

where s_a is the sum of the gravity and external acceleration of the tracking object, s_{a_r} is the sum of the gravity and external acceleration, s_{a_b} is the accelerometer bias that models its derivative by a Gauss-Markov noise, s_{a_n} is the accelerometer white noise.

3.3. *Magnetometer*

The magnetometer measures the magnetic field of the tracking object in μT. It is represented as $s_m = [s_{m_x} \quad s_{m_y} \quad s_{m_z}]^T$. The Earth's magnetic field is modeled by a dipole and follows the basic laws of magnetic fields, i.e., at any location the Earth's magnetic field can be represented by a three-dimensional vector. More information is provided in.[37]

The three types of noise of the magnetometer are:

- angle random walk
- bias instability
- correlated noise

The continuous time model of the magnetometer is as follows:

$$s_m = s_{m_r} + s_{m_b} + s_{m_n} \tag{3}$$

where s_m is the magnetic field measured by the magnetometer, s_{m_r} is the true magnetic field, s_{m_b} is the bias of the magnetometer where its derivate is modeled by a Gauss-Markov noise, and s_{m_n} is the white noise.

The magnetometer not only measures the Earth's magnetic field but is also influenced by magnetic disturbances caused by ferromagnetic objects in the environment.

4. Attitude Estimation Algorithm: Madgwick Filter

Attitude estimation algorithms are described using common notations used for quaternion and sensor readings. The estimated vector v is described by $\hat{v} = [\hat{v}_x \quad \hat{v}_y \quad \hat{v}_z]^T$, the quaternion and angular rate errors are given by q_e, w_e, and the time difference between 2 epochs is $\triangle t$.

An attitude estimation algorithm use two reference vectors E_a and E_m in order to estimate q. In a noise-free environment, the relation between these two reference vectors are given as:

$$s_{a_q} = q^{-1} \otimes E_{a_q} \otimes q \tag{4}$$

where $\otimes$ is the quaternion multiplication.[29] s_{a_q} is the quaternion form of s_a, which can be written as $S_{a_q} = [0 \quad s_{a_x} \quad s_{a_y} \quad s_{a_z}]^T$. E_{a_q} is the quaternion form of E_a. For the static case it is $E_a = [0 \quad 0 \quad g]^T$ where g is the acceleration due to gravity ($g \approx 9.8\frac{m}{s^2}$).

In a noise-free environment without any magnetic deviation, the relation between E_m and s_m is as follows:

$$s_{m_q} = q^{-1} \otimes E_{m_q} \otimes q \tag{5}$$

where s_{m_q} is the quaternion form of s_m, which can be written as $s_{m_q} = [0 \quad s_{m_x} \quad s_{m_y} \quad S_{m_z}]^T$. E_{m_q} is the quaternion form of E_m. If there are no magnetic deviations, E_m can be calculated using.[34]

The angular velocity measurements from a gyroscope to describe the variations of the attitude in terms of quaternions are given as such:

$$\dot{q} = \frac{1}{2} q \otimes s_{w_q} \tag{6}$$

where s_{w_q} is the quaternion of s_w.

The Madgwick filter is a gradient descent based algorithm where the quaternion error from the gradient descent algorithm provides also a gyroscope drift compensation. The algorithm is shown in Algorithm 1. In the algorithm, J_t refers to the Jacobian Matrix of F_t, β is the divergence rate of q_t representing the magnitude of a quaternion derivative corresponding to the gyroscope measurement error, and ζ is the integral gain.

Algorithm 1 Madgwick Filter [33]

$$E_{\hat{h}_{q,t}} = \hat{q}_{t-1} \otimes s_{m_{q,t}} \otimes \hat{q}_{t-1}^{-1}$$

$$E_{\hat{m}_{q,t}} = [0 \quad 0 \quad \sqrt{E_{\hat{h}_{x,t}}^2 + E_{\hat{h}_{y,t}}^2} \quad E_{\hat{h}_{z,t}}]^T$$

$$F_t = \begin{bmatrix} \hat{q}_{t-1}^{-1} \otimes E_{a_{q,t}} \otimes \hat{q}_{t-1} - s_{a_{q,t}} \\ \hat{q}_{t-1}^{-1} \otimes E_{m_{q,t}} \otimes \hat{q}_{t-1} - s_{m_{q,t}} \end{bmatrix}$$

$$\hat{q}_{e,t} = J_t^T F_t$$

$$s_{\hat{w}_{e,t}} = 2\hat{q}_{t-1} \otimes \hat{q}_{e,t}$$

$$s_{\hat{w}_{b,t}} = s_{w_{e,t}}$$

$$s_{\hat{w}_t} = s_{w_t} - \zeta s_{w_{b,t}}$$

$$\dot{\hat{q}}_t = \frac{1}{2}\hat{q}_{t-1} \otimes s_{\hat{w}_{q,t}} - \beta \frac{\hat{q}_{e,t}}{||\hat{q}_{e,t}||}$$

Fig. 1. Block diagram of Madgwick Filter[32]

Figure 2 shows the block diagram of the Madgwick filter whereby two main processes are used to compute the orientation of the rigid body. First, the alignment of the gyroscope measurements depending on the parameter is done via a correction algorithm. During quaternion propagation and in order to minimize the effects that are due to the bias and the drift error, both are used to compute the body orientation obtained from the orientation estimated at the previous step. Then, the accelerometer and magnetometer measurements are fused together using a adjustable parameter, β, using a gradient descent algorithm that is described in.[30] The output of this algorithm is then used to correct the orientation estimated considering only the gyroscope measurements.

5. MIMU Simulation Configuration Experiments

The code was implemented using Matlab version R2017A. The machine used for the experiments consisted of a 16-core/32-thread machine with Intel(R) Xeon(R) CPU E5-2680 @ 2.70GHz with 32GB of RAM.

The data used was obtained from.[35] The foot mounted MIMU measurement data contains sensor data of a straight trajectory of 1,000 steps. The steps are based on a human step pattern characteristics measured by a motion capture system. The data collected from the MIMU is the acceleration, turn rates from the gyroscope and the magnetic field. The data set includes ground truth values of the orientation (Euler and DCM). The units are in meters, seconds and radians. The sampling frequency used was 100 Hz, and gravity is given as $9.8\frac{m}{s^2}$. The MIMU sensor was the XSense Mti which has the following specification:

- Accelerometer: $0.012\frac{m}{s^2}$ standard deviation random noise and a random constant with a Gaussian distribution and a standard deviation of $0.04\frac{m}{s^2}$ for the bias.
- Gyroscope: $0.0087\frac{rad}{s}$ standard deviation random noise and a random constant with a Gaussian distribution and a standard deviation of $0.015\frac{rad}{s}$ for the bias.

XSense MIMU are seen as the gold standard for scientific research and are commonly used in motion sensing applications[36]-.[39]

Figure 3 shows the sensor data obtained. It outlines the gyroscope, accelerometer, and magnetometer data and shows the cyclic steps of the walking motion.

5.1. *Simulation Experiments*

For the evaluation, the following experiments were run to:

(1) Investigate the RMSE values for increasing numbers of sensors;
(2) Investigate the execution time for the sequential execution of the code (normal implementation) for increasing numbers of sensors;
(3) Investigate the execution time for the parallel execution of the code for increasing numbers of sensors including multiples of 16 (since we have 16 cores available on the machine).

5.1.1. *Investigation of RMSE Values for Increasing Numbers of Sensors*

First, we ran the Madgwick AHRS implementation and observed the RMSE (Root Mean Square Error) values of the estimated Euler angles in x-, y-, and z-direction with increasing numbers of sensors starting from one sensor up to 16 sensors. Figure 4 shows the RMSE values exponentially decreasing for all three axes with increasing numbers of sensors. However, the Y axis is the least affected and remains more or less unchanged since we are working with foot data. The movement is primarily in the X and Z direction but since the terrain is flat the y-axis remains more or less constant.

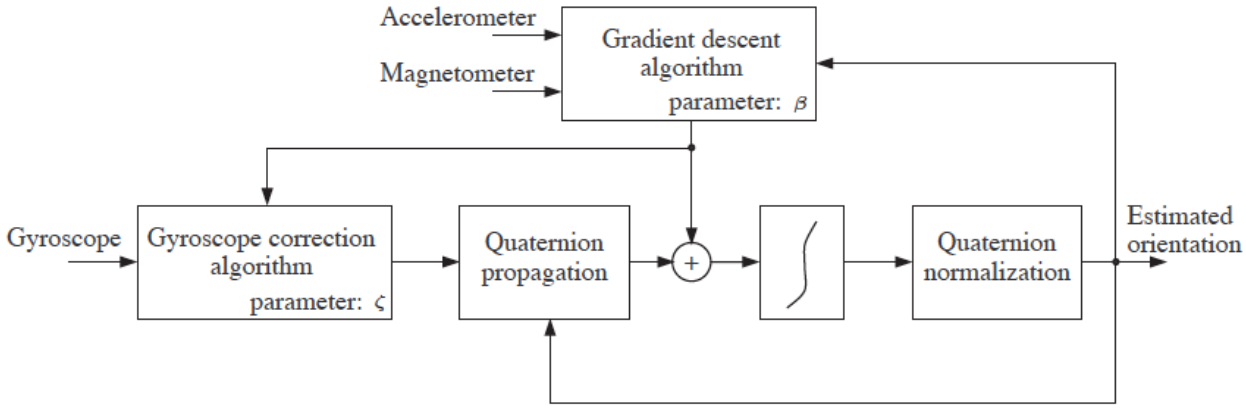

Fig. 2. Block diagram of Madgwick Filter[32]

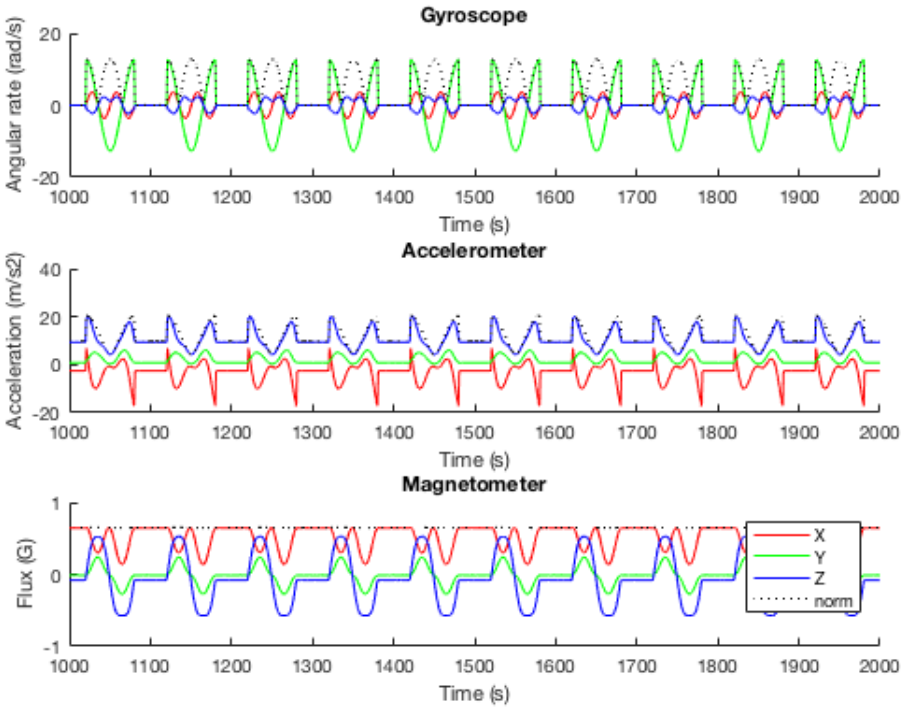

Fig. 3. Sensor data of gyroscope, accelerometer, magnetometer

Figure 5 shows the norm RMSE based on the three RMSE values of the three directions. The exponential trend of the norm RMSE is well observed.

Table 1 tabulates the results as plotted in Figure 4 and Figure 5.

Based on the norm RMSE values, the relative improvement can be calculated as shown in Table 2. The relative improvement using 2 sensors is 11.54% whereas an improvement of 26.01% is achieved using 16 sensors. The exponential downward trend seen in the norm RMSE values can also be observed by the relative improvement values for increasing numbers of sensors.

5.1.2. *Investigation of Execution Time*

During the simulation experiments we observed that the running time increases exponentially with the increase in the number of sensors; Figure 6 shows this trend. For ex-

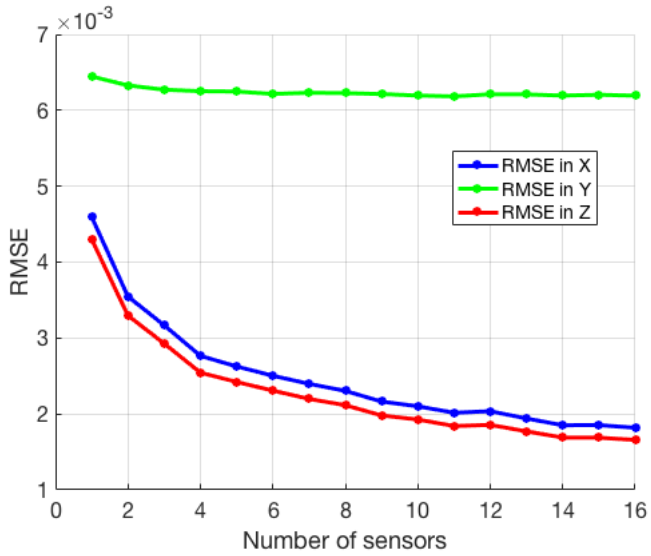

Fig. 4. RMSE values in X, Y, and Z direction with increasing numbers of sensors

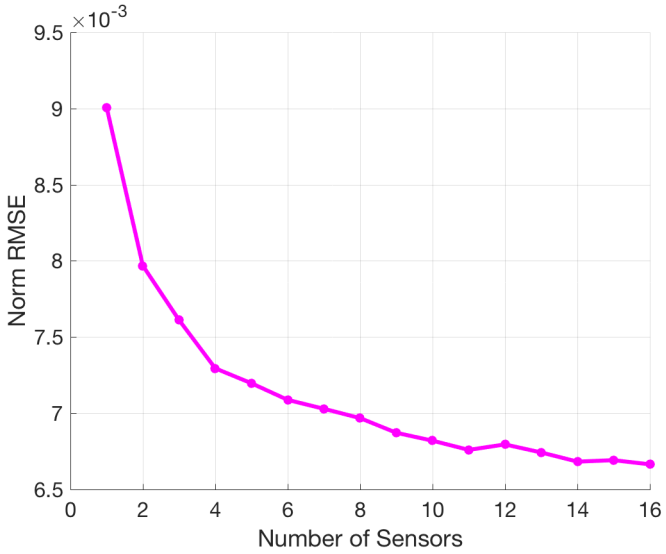

Fig. 5. Norm RMSE value with increasing numbers of sensors

ample, the running time using one sensor is 15.1 seconds whereas the running time using 20 sensors is 868.8 seconds.

The exponential trend of the execution times for increasing numbers of sensors led us to parallelize the simulation code and move away from the sequential execution to a parallel execution to estimate the euler angles. Figure 7 shows the sequential and parallel execution times with increasing numbers of sensors. As can be seen by the figure, the parallel execution time is quite steady rising from 13.5 seconds using 1 sensor up to 37.1 seconds for 20 sensors. Compared to the sequential version this rise is negligible given that the running time using 20 sensors was 868.8 seconds for the sequential version. The obtained values are also provided in Table 3 for completeness.

Zooming in on the parallel execution times, as shown in Figure 8, we can observe also an exponential trend, however, nothing compared to the sequential execution time trend. The execution time using two sensors is 27.4 seconds using sixteen sensors. The reason for the exponential trend is that the sequential portion of the code has a higher impact than the parallel portion of the code with larger numbers of sensors used.

In order to perform a scalability analysis on how well the parallel implementation fares we ran simulations with multiples of 16 sensors (from 16 to 160 sensors) to observe the trend in the execution time of the parallel implemen-

Table 1. RMSE in X, Y, and Z direction and norm RMSE with increasing numbers of sensors

Number of sensors	RMSE_X	RMSE_Y	RMSE_Z	norm RMSE
1	0.0045940	0.0064458	0.0042995	0.0090077
2	0.0035468	0.0063283	0.0032958	0.0079680
3	0.0031680	0.0062713	0.0029274	0.0076115
4	0.0027652	0.0062521	0.0025443	0.0072944
5	0.0026259	0.0062473	0.0024215	0.0071964
6	0.0025034	0.0062161	0.0023076	0.0070874
7	0.0023966	0.0062313	0.0021983	0.0070289
8	0.0023042	0.0062262	0.0021151	0.0069677
9	0.0021632	0.0062143	0.0019802	0.0068715
10	0.0021009	0.0061950	0.0019270	0.0068195
11	0.0020160	0.0061833	0.0018408	0.0067591
12	0.0020363	0.0062115	0.0018560	0.0067951
13	0.0019402	0.0062095	0.0017707	0.0067422
14	0.0018520	0.0061940	0.0016896	0.0066821
15	0.0018529	0.0062048	0.0016870	0.0066917
16	0.0018191	0.0061931	0.0016584	0.0066644

Table 2. Relative improvement in RMSE with increasing number of sensors

Number of sensors	1	2	3	4	5	6	7	8	9	10
Improvement	-	11.54	15.50	19.02	20.11	21.32	21.97	22.65	23.72	24.29
Number of sensors	11	12	13	14	15	16	17	18	19	20
Improvement	24.96	24.56	25.15	25.82	25.71	26.01	25.83	26.59	26.52	26.39

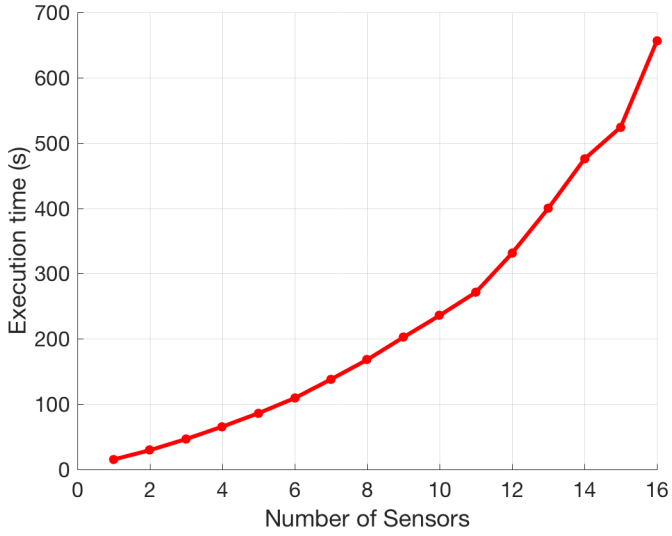

Fig. 6. Execution time of increasing numbers of sensors - sequential version

tation further. Figure 9 shows the results; the execution times in double logarithmic scale show a linear trend for

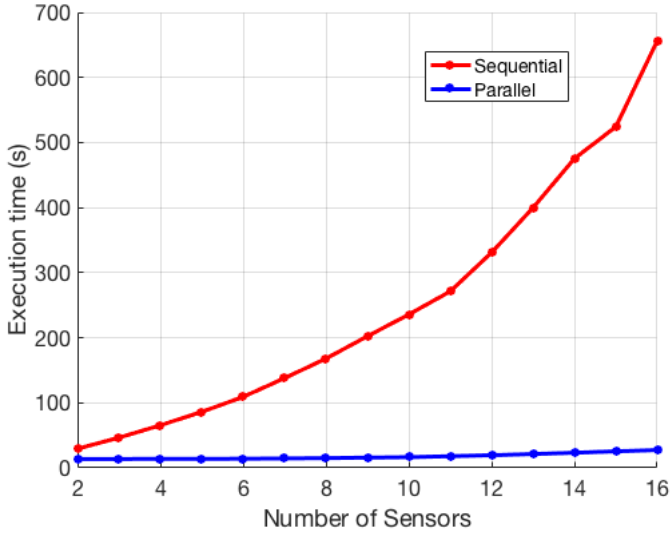

Fig. 7. Execution time of increasing numbers of sensors - sequential versus parallel version

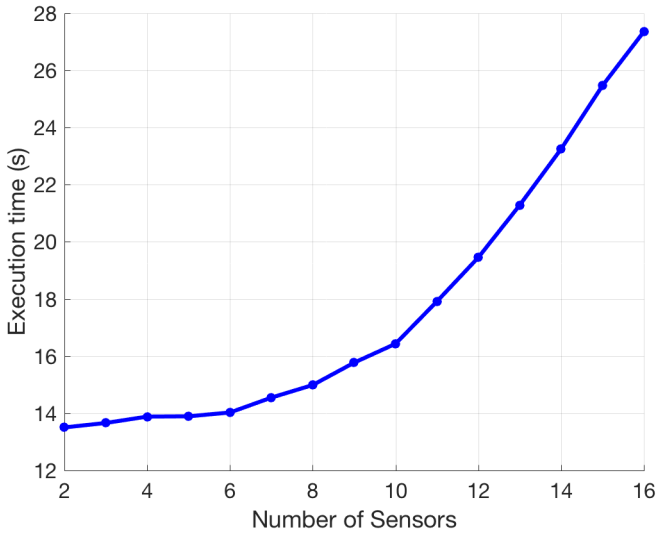

Fig. 8. Execution time of increasing numbers of sensors - parallel version

the multiples of 16 sensors from 32 sensors onwards. Given the improved execution times using the parallel implementation this makes it suitable for real-time execution.

6. Conclusion

Past research has shown that redundant MIMUs are an efficient way to improve navigation performances for example for unmanned air vehicles. However, the precise relationship between the number of sensors employed and the accuracy enhancement remains unclear and none of the research work offers guidance as to how many sensors are required to achieve a specific accuracy.

This paper evaluated different MIMU sensor array configurations by scaling the numbers of sensors used. Simulation experiments were carried out using ground truth acceleration, rotation, and magnetometer data. The evaluation was done using the readings from each sensor in the virtual frame averaged from the resulting accelerometer, gyroscope, and magnetometer and fused by the Madgwick filter to obtain an orientation estimate. A root mean square error (RMSE) was calculated based on the estimated Euler angles and compared to the orientation RMSE of a single MIMU centered at the origin of the system.

The simulation experiments revealed the following.

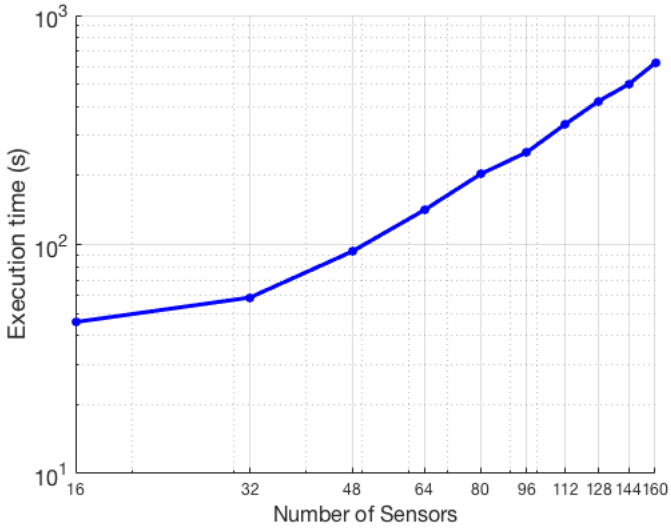

Fig. 9. Execution time of multiples of 16 sensor increments - parallel version (in double log scale)

Table 3. Execution times in seconds for sequential and parallel version

Sensors	1	2	3	4	5	6	7	8
Sequential	15.10	29.41	46.43	65.44	86.06	109.12	137.88	167.92
Parallel	13.48	13.50	13.66	13.88	13.89	14.03	14.55	14.99
Sensors	9	10	11	12	13	14	15	16
Sequential	202.27	235.70	271.15	330.93	399.70	475.34	524.09	655.98
Parallel	15.77	16.43	17.91	19.45	21.28	23.25	25.47	27.36

Based on the norm RMSE values, the relative improvement using 2 sensors is 11.54% whereas an improvement of 26.01% is achieved using 16 sensors. However, we observed that the execution time exponentially increases with every sensor added to the orientation estimation. Thus, a parallel version using a multi-core machine was designed and implemented. A speedup analysis was performed to measure the performance gain in terms of execution time. Using a 16-core machine and running the orientation estimation using the Madgwick filter, the findings of the sixteen sensor configuration were that the execution time is less than twice the execution time of running a one-sensor configuration, and 24 times less than using the sequential version with the added benefit of a 26% increase in accuracy.

References

[1] H. Zhao and Z. Y. Wang, Motion measurement using inertial sensors, ultrasonic sensors, and magnetometers with extended Kalman filter for data fusion, IEEE Sensors Journal, vol. 12, no. 5, pp. 943-953, May 2012.

[2] M. Tanenhaus, D. Carhoun, T. Geis, E. Wan, and A. Holland, Miniature IMU/INS with optimally fused low drift MEMS Gyro and accelerometers for applications in GPS-denied environments, in Proc. IEEE/ION PLANS 2012, Myrtle Beach, South Carolina , April 2012, pp. 259-264.

[3] R. Zhu and Z. Zhou, A real-time articulated human motion tracking using tri-axis inertial/magnetic sensors package, IEEE Trans. Neural Syst. Rehabil. Eng., vol. 12, no. 2, pp. 295-302, June 2004.

[4] H. Chao, A. M. Jensen, Y. Han, Y. Q. Chen, and M. McKee, Advances in Geoscience and Remote Sensing. Vukovar, Croatia: IN-TECH, 2009, ch. AggieAir: Towards Low-cost Cooperative Multispectral Remote Sensing Using Small Unmanned Aircraft Systems.

[5] H. Chao, M. Baumann, A. M. Jensen, Y. Q. Chen, Y. Cao, W. Ren, and M. McKee, Band-reconfigurable multi-UAV-based cooperative remote sensing for real-time water management and distributed irrigation control, in Proceedings of the International Federal of Automatic Control (IFAC) World Congress, July 2008, pp. 11, 744-11 749.

[6] Q. Feng, J. Liu, J. Gong, UAV Remote Sensing for Urban Vegetation Mapping Using Random Forest and

Texture Analysis. Remote Sens. 2015, 7, 1074-1094.

[7] S. Chen, S. Guo, Y. Li, Real-time tracking a ground moving target in complex indoor and outdoor environments with UAV. In Proceedings of the IEEE International Conference on Information and Automation (ICIA), Ningbo, China, 1-3 August 2016; pp. 362-367.

[8] T. Kobayashi, S. Seimiya, K. Harada, M. Noi, Z. Barker, G. Woodward, A. Willig, R. Kohno, Wireless technologies to assist search and localization of victims of wide-scale natural disasters by unmanned aerial vehicles. In Proceedings of the International Symposium on Wireless Personal Multimedia Communications (WPMC), Bali, Indonesia, 17-20 December 2017; pp. 404-410.

[9] K. Wu, T. Gregory, J. Moore, B. Hooper, D. Lewis, Z. Tse, Development of an indoor guidance system for unmanned aerial vehicles with power industry applications. IET Radar Sonar Navig. 2017, 11, 212-218.

[10] A. J. Kerns, D. P. Shepard, J. A. Bhatti, and T. E. Humphreys, Unmanned aircraft capture and control via GPS spoofing, Journal of Field Robotics, vol. 31, no. 4, pp. 617-636, 2014.

[11] E. Munoz Diaz, O. Heirich, M. Khider, P. Robertson, Optimal sampling frequency and bias error modeling for foot-mounted IMUs, 2013 International Conference on Indoor Positioning and Indoor Navigation (IPIN), Montbeliard-Belfort, France, 2013.

[12] A. Lennartsson, D. Skoogh, Sensor redundancy for inertial navigation, Technical report, FOI (Swedish Defense Research Agency), SE, 2003.

[13] S. Sukkarieh, P. Gibbens, B. Grocholsky, K. Willis, H. Durrant Whyte, A low-cost, redundant inertial measurement unit for unmanned air vehicles, Int. J. Robot. Res. 19(11), 1089-1103, 2000.

[14] M. Jafari, Optimal redundant sensor configuration for accuracy increasing in space inertial navigation system, Aerospace Science and Technology, Volume 47, December 2015.

[15] H. Martin, P. Groves, M. Newman, R. Faragher, A New Approach to Better Low-Cost MEMS IMU Performance Using Sensor Arrays, Proceedings of the 26th International Technical Meeting of The Satellite Division of the Institute of Navigation (ION GNSS 2013), Nashville, TX, USA, 2013.

[16] A. Waegli, S. Guerrier, and J. Skaloud, Redundant MEMS-IMU integrated with GPS for Performance Assessment in Sports, in Proceedings of the IEEE/ION PLANS 2008, Monterey, CA, USA, 2008.

[17] J. Crassidis, J. Markley, and Y. Cheng, Nonlinear attitude filtering methods, AIAA Journal of Guidance, Control, and Dynamics, vol. 30, no. 1, pp. 12-28, 2007.

[18] S.-G. Kim, J. Crassidis, Y. Cheng, and A. M. Fosbury, Kalman filtering for relative spacecraft attitude and position estimation, AIAA Journal of Guidance, Control, and Dynamics, vol. 30, no. 1, pp. 133-143, 2007.

[19] R. Mahony, T. Hamel, and J.-M. Pflimlin, Non-linear complementary filters on the special orthogonal group, IEEE Transactions on Automatic Control, vol. 53, no. 5, pp. 1203-1218, 2008.

[20] R. W. Beard, Studies in Computational Intelligence. Springer Verlag, Berlin Heidelberg, 2007, vol. 70, ch. State Estimation for Micro Air Vehicles, pp. 173-199.

[21] D. B. Kingston and R. W. Beard, Real-time attitude and position estimation for small UAVs using low-cost sensors, in Proceedings of the AIAA 3rd Unmanned Unlimited Systems Conference and Workshop, no. AIAA-2007-6514, Chicago, IL, Sep. 2004.

[22] J. S. Jang and D. Liccardo, Small UAV automation using MEMS, IEEE Aerospace and Electronic Systems Magazine, vol. 22, no. 5, pp. 30-34, 2007.

[23] S. Bonnabel, P. Martin, and P. Rouchon, Symmetry-preserving observers, IEEE Transactions on Automatic Control, vol. 53, no. 11, pp. 2514-2526, 2008.

[24] S. A. Ludwig, K. D. Burnham, A. R. Jimenez, P. A. Touma, Comparison of attitude and heading reference systems using foot mounted MIMU sensor data: basic, Madgwick, and Mahony, Proceedings of SPIE Conference on Sensors and Smart Structures Technologies for Civil, Mechanical, and Aerospace Systems, Denver, CO, USA, March 2018.

[25] S. A. Ludwig, K. D. Burnham, Comparison of Euler Estimate using Extended Kalman Filter, Madgwick and Mahony on Quadcopter Flight Data, 2018 International Conference on Unmanned Aircraft Systems (ICUAS'18), Dallas, Texas, USA, June 2018.

[26] S. A. Ludwig, Genetic Algorithm based Kalman Filter Adaptation Algorithm for Magnetic and Inertial Measurement Unit, 2018 IEEE Congress on Evolutionary Computation, Rio de Janeiro, Brazil, July 2018.

[27] S. Guerrier, Improving Accuracy with Multiple Sensors: Study of Redundant MEMS-IMU/GPS Configurations, Proceedings of the 22Nd International Technical Meeting Of The Satellite Division Of The Institute Of Navigation, 2009.

[28] S. Guerrier, Integration of Skew-Redundant MEMS-IMU with GPS for Improved Navigation Performance, Master's thesis, EPFL, 2008.

[29] A. Waegli, Trajectory Determination and Analysis in Sports by Satellite and Inertial Navigation, Ph.D. dissertation, Thesis 4288, EPFL, 2009.

[30] S. Sukkarieh, P. Gibbens, B. Brocholsky, K. Willis, and H. Durrant-Whyte, A Low-Cost Redundant Inertial Measurement Unit for Unmanned Air Vehicles, The International Journal of Robotics Research, vol. 19, no. 11, pp. 1089-1103, 2000.

[31] A. Osman, B. Wright, S. Nassar, A. Noureldin, and N. El-Sheimy, Multi-Sensor Inertial Navigation Systems Employing Skewed Redundant Inertial Sensors, in Proceedings of the ION GNSS 2006, Fort Worth, TX, USA, 2006.

[32] T. Michel, H. Fourati, P. Geneves, N. Layada. A Comparative Analysis of Attitude Estimation for Pedestrian Navigation with Smartphones. 2015 International Conference on Indoor Positioning and Indoor Navigation, Banff, Canada, October 2015.

[33] S. O. Madgwick, A. J. Harrison, and R. Vaidyanathan, Estimation of IMU and MARG orientation using a gradient descent algorithm, in 2011 IEEE International Conference on Rehabilitation Robotics (ICORR), 2011.

[34] NGA and the U.K.'s Defence Geographic Centre (DGC), The world magnetic model, `http://www.ngdc.noaa.gov/geomag/WMM`, 2015, [Online; last accessed December 2017].

[35] Foot Mounted IMU data sets for the evaluation of PDR algorithms, LOPSI Research group, Spain, `http://lopsi.weebly.com/downloads.html`, 2017.

[36] A. G. Cutti, A. Giovanardi, L. Rocchi, A. Davalli, R. Sacchetti, Ambulatory measurement of shoulder and elbow kinematics through inertial and magnetic sensors. Med. Boil. Eng. Comput., 46, 169-178, 2008.

[37] W. M. Chung, S. Yeung, W. W. Chan, R. Lee, Validity of VICON Motion Analysis System for Upper Limb Kinematic Measurement - A Comparison Study with Inertial Tracking Xsens System. Hong Kong Physiother. J. 2011.

[38] D. Hamacher, D. Bertram, C. Folsch, L. Schega, Evaluation of a visual feedback system in gait retraining: A pilot study. Gait Posture, 36, 182-186, 2012.

[39] K. Saber-Sheikh, E. C. Bryant, C. Glazzard, A. Hamel, R. Y. Lee, Feasibility of using inertial sensors to assess human movement. Man. Ther., 15, 122-125, 2010.